

1 **Trim7 does not have a role in the restriction of murine norovirus infection in vivo**

2

3 Mridula Annaswamy Srinivas¹, Linley R. Pierce¹, Mikayla C. Olson¹, Shelly J.
4 Roberston², Gail L. Sturdevant², Sonja M. Best², Robert C. Orchard^{1,3#}

5

6 1 Department of Immunology, University of Texas Southwestern Medical Center, Dallas,
7 TX, USA

8 2 Laboratory of Neurological Infections and Immunity, Rocky Mountain Laboratories,
9 National Institute of Allergy and Infectious Diseases, National Institutes of Health,
10 Hamilton MT, USA

11 3 Department of Microbiology, University of Texas Southwestern Medical Center, Dallas,
12 TX, USA

13

14 **# Correspondence to:** Robert.Orchard@utsouthwestern.edu (R.C.O.)

15

16

17 **Abstract**

18 Trim7 is an E3 ubiquitin ligase that was recently identified as a central regulator of host-
19 viral interactions with both pro-viral and anti-viral activity in cell culture. As an inhibitor,
20 Trim7 overexpression ubiquitinates viral proteins by recognizing C-terminal glutamines
21 that are hallmarks of 3C-like protease cleavage events. Here we sought to determine the
22 physiological impact of Trim7 in resolving murine norovirus (MNV) infection of mice as
23 MNV is potently inhibited by Trim7 in vitro. Utilizing two independently derived Trim7
24 deficient mouse lines we found no changes in the viral burden or tissue distribution of
25 MNV in both an acute and persistent model of infection. Additionally, no changes in
26 cytokine responses were observed after acute MNV infection of Trim7-deficient mice.
27 Furthermore, removal of potentially confounding innate immune responses such as
28 STING and STAT1 did not reveal any role for Trim7 in regulating MNV replication. Taken
29 together, our data fails to find a physiological role for Trim7 in regulating MNV infection
30 outcomes in mice and serves as a caution for defining Trim7 as a broad acting antiviral.

31

32 **Importance**

33 Intrinsic antiviral molecules that restrict viral replication are important drivers of viral
34 evolution and viral tropism. Recently, Trim7 was shown to provide cell intrinsic protection
35 against RNA viruses, including murine norovirus. Biochemically, Trim7 recognizes the
36 cleavage product of viral proteases, suggesting a novel and broad mechanism to restrict
37 viral replication. Here, we tested whether Trim7 had a physiological role in restricting
38 murine norovirus replication in mice. Unexpectedly, we found no impact of viral replication
39 or innate immune responses during murine norovirus infection. Our findings urge caution
40 in defining Trim7 as a broad antiviral factor in the absence of in vivo evidence.

41 **Introduction**

42 Noroviruses are non-enveloped positive-sense single stranded RNA viruses that are a
43 leading cause of infectious gastroenteritis worldwide^{1,2}. Norovirus infections in humans
44 are typically self-resolving but cause a significant economic burden³. Children and
45 immunocompromised individuals can be affected by more severe, recurrent and
46 persistent infections^{4,5}. Despite their high infectivity and burden, there is currently no
47 vaccine or treatment for noroviral gastroenteritis due to difficulties in culturing human
48 noroviruses (HNoV). Stem-cell derived enteroid cultures enable growth of HNoV in vitro
49 and hold promise to accelerate therapeutic discoveries⁶⁻⁹. However, there are no
50 accessible small animal models to study HNoV infections in vivo¹⁰. Murine norovirus
51 (MNV) has emerged as a model system to study HNoV due to its ability to infect mice and
52 replicate in standard cell culture conditions¹¹⁻¹³. The MNV model system is a robust
53 platform to study host-virus interactions and immune factors against noroviruses in a
54 natural setting.

55 Previously, we identified a host protein Tripartite motif-containing protein 7 (Trim7) as a
56 strong antiviral protein against MNV replication¹⁴. Trim7 is an E3 ubiquitin ligase that was
57 originally described as an interactor of glycogenin¹⁵. Trim7 preferentially binds and
58 ubiquitinates substrates with a C-terminal glutamine residue¹⁶⁻¹⁸. In recent years, Trim7
59 has been widely studied for its role in viral replication and host defense systems with
60 reports of both proviral and antiviral activities. For example, Trim7 ubiquitinates Zika virus
61 envelope protein E, enhancing viral entry into host cells¹⁹. Others report that Trim7
62 ubiquitinates stimulator of interferon genes (STING) and mitochondrial antiviral signaling
63 protein (MAVS) leading to a reduced innate immune response and decreased protection

64 against infection^{20,21}. Contrastingly, Trim7 has antiviral activity towards enteroviruses via
65 ubiquitination of non-structural protein 2BC of coxsackievirus CVB3²². The CVB3 3C
66 protease cleaves Trim7 to antagonize its antiviral function²³. With respect to noroviruses,
67 we and others have further demonstrated by infection and biochemical studies that Trim7
68 can target norovirus non-structural proteins NS6 and NS3^{17,18,24}. 3C-like viral proteases
69 preferentially cleave substrates at a glutamine residue²⁵, placing a potential for Trim7 to
70 be a broad regulator of 3C-protease cleavage products. However, the antiviral role of
71 Trim7 in the physiological setting has not been tested. Given the complex relationship
72 between pro- and anti-viral facets of Trim7 biology, it is important to define how this protein
73 at the nexus of intrinsic immunity impacts viral infection in vivo.

74 MNV strains have disparate infection outcomes in mice that have been used to model
75 different aspects of HNoV infections^{11,12}. Certain strains of MNV such as MNV^{CW3} cause
76 an acute infection of both intestinal and extraintestinal tissues via infection of immune
77 cells^{26,27}. These infections are typically self-resolving but can persist in the absence of the
78 adaptive immune system and are lethal in interferon deficient settings, such as STAT1^{-/-}
79 mice^{12,28}. Acute infections by MNV have been used to model the acute phase of HNoV
80 infections. In contrast, some strains of MNV establish a persistent, enteric infection that
81 is confined to the gastrointestinal tract²⁹. The prototypical persistent strain MNV^{CR6} infects
82 tuft cells and evades both innate and adaptive immunity through mechanisms that are still
83 not well understood³⁰⁻³⁶. Persistent MNV infections mirror the long-term, asymptomatic
84 shedding observed for HNoV³⁷. The diversity of MNV phenotypes provides not only an
85 opportunity to explore different properties of norovirus pathogenesis but also the role of
86 host factors such as Trim7 in restricting MNV in a cell or tissue specific manner.

87

88 To determine the physiological impact of Trim7 in resolving both acute and persistent
89 norovirus infections in mice, we utilized two independently derived Trim7 deficient mouse
90 lines. Despite robust restriction of MNV in vitro by overexpressed Trim7, we fail to observe
91 any change in MNV replication in Trim7 deficient mice. Furthermore, no changes in
92 cytokine production were observed during MNV infection when Trim7 was absent.
93 Elimination of potentially confounding immune pathways such as STAT1 or STING did
94 not reveal any physiological role for Trim7 in restricting MNV replication. While Trim7 may
95 play an important role in a yet to be tested MNV infection system, caution is urged in
96 defining Trim7 as a broad acting antiviral recognizing the products of 3C-like protease
97 cleavage events.

98 **Results**

99 **Generation of Trim7 knockout mouse lines**

100 To assess the role of Trim7 in vivo, we acquired two independent Trim7 deficient mouse
101 lines to circumvent the challenges in detecting endogenous Trim7 protein expression. The
102 first line (BL6/Trim^{+1/+1}) has a single nucleotide insertion in exon 1 leading to a premature
103 stop codon and has been previously characterized¹⁹ (**Figure 1A**). For added rigor, we
104 generated a second Trim7 mouse with a 12kb deletion spanning exons 1 through 7 of
105 Trim7 (BL6ΔTrim7; **Figure 1A**). We have not been able to robustly and reproducibly
106 detect endogenous Trim7 via antibodies from multiple manufacturers in any of our mouse
107 lines or tissues (data not shown). **Figure 1B** is a representative example with one of these
108 antibodies demonstrating a failure to detect a specific Trim7 band. Thus, we designed a
109 qRT-PCR assay targeting exon 1 of Trim7 to determine the tissue distribution of Trim7 in
110 wild-type mice (**Figure 1A**). Consistent with previous results^{19,22}, we detect high levels of
111 Trim7 in the heart, leg muscle, and kidney (**Figure 1C**). We then examined the expression
112 level of Trim7 at sites where MNV replicates. Our data demonstrates low, but detectable
113 levels of Trim7 in the ileum and colon while higher levels at extraintestinal sites like the
114 spleen, liver, and lung (**Figure 1C**). Using this qRT-PCR assay we also confirmed the loss
115 of RNA expression of Trim7 in the BL6ΔTrim7 mice (**Figure 1D**).

116

117 **No detectable role for Trim7 in restriction of acute murine norovirus infection in**
118 **vivo**

119 We first tested whether endogenous Trim7 restricts acute, systematic norovirus infection
120 in vivo. We inoculated WT BL6 and BL6/Trim7^{+1/+1} littermates with MNV^{CW3} and harvested
121 tissues 7 days post-infection. Consistent with previous results, we find MNV genomes in
122 mesenteric lymph nodes (MLN), spleen, and liver in wild-type mice (**Figure 2A**). MNV^{CW3}
123 does not infect the colon and poorly infects the ileum. Deficiency of Trim7 in the infected
124 mice does not alter the sites of infection or the burden of MNV in these mice (**Figure 2A**).
125 We also found similar results comparing BL6ΔTrim7 heterozygous and knockout
126 littermates infected with MNV^{CW3} (**Figure 2B**). Overall, these data fail to demonstrate an
127 impact of Trim7 on acute MNV replication in vivo.

128

129 **No impact of Trim7 on MNV persistence in gastro-intestinal tissues**

130 Persistent strains of MNV have a distinct tropism of tuft cells thus Trim7 may have an
131 impact on persistent strains rather than acute strains^{29,33,34}. To evaluate the impact of
132 Trim7 on the gastro-intestinal tissue infection and persistence of MNV, we infected WT
133 and BL6/Trim7^{+1/+1} littermate-matched mice with MNV^{CR6} and monitored viral load over
134 21 days of infection. We confirmed successful infection, replication, and persistence of
135 MNV infection in these mice by determining viral load in the feces from day 3 to day 21
136 post-infection (**Figure 3A**). Trim7 deficiency had no impact on fecal shedding at either
137 early or persistent time points (**Figure 3A**). The colon and MLN harbor high levels of
138 MNV^{CR6} and Trim7 deficiency did not alter the amount of virus detected at these sites
139 (**Figure 3B and 3C**). MNV^{CR6} does not robustly infect the ileum, spleen, or liver of
140 immunocompetent animals²⁹. BL6/Trim7^{+1/+1} animals had similarly low or undetectable
141 amounts of MNV genomes in these tissues as compared to their Trim7 sufficient littermate

142 controls (**Figure 3D-3F**). Taken together these data suggest that Trim7 has no impact on
143 gastrointestinal infection and persistent by MNV^{CR6}, nor does Trim7 deficiency enable a
144 new tissue niche at persistent time points.

145

146 **Trim7 does not impact innate immune response to acute MNV infection**

147 Previous studies have shown that Trim7 inhibits innate immune responses by regulating
148 the expression of innate immune sensors STING and MAVS^{20,21}. In these studies, Trim7
149 deficient mice infected with RNA or DNA viruses produced more type I interferons and
150 other pro-inflammatory cytokines and chemokines like TNF- α , IFN- β , Cxcl10 and
151 ISG56^{20,21}. MNV infection also leads to interferon stimulation and upregulation of
152 cytokine/chemokine responses^{12,41,42}. We investigated the innate immune response to
153 MNV^{CW3} infection in MLN, spleen and liver of BL6/Trim7^{+1/+1} mice at 7 days post-infection
154 by measuring the induction of cytokines via qPCR. No significant differences were
155 observed in the transcript levels of IFN- β 1, IL-6, Ifit1 or Cxcl10 in any of the tested tissues
156 between infected BL6/Trim7^{WT/WT} and BL6/Trim7^{+1/+1} mice (**Figure 4A-4D**). These data
157 indicate that Trim7 does not impact the innate immune response to acute MNV infection.

158

159 **STING and STAT1 dependent innate pathways do not mask a role of Trim7 in** 160 **restricting acute MNV infection**

161 MNV can activate the cGAS/STING pathway by inducing the release of mitochondrial
162 DNA from infected cells which in turn can restrict MNV replication in vitro. Whether this
163 pathway is relevant to MNV infection in mice has not been evaluated^{43,44}. Trim7 has been

164 reported to target STING for ubiquitination and degradation, thus serving as a proviral
165 factor for viruses²¹. Consequently, it is possible that the physiological effect of Trim7 is
166 masked by the greater impact of Trim7 regulation of STING-mediated restriction of MNV.
167 To eliminate this possible confounding pathway, we crossed the BL6/Trim7^{+1/+1} mice onto
168 a STING^{Gt/Gt} background. In doing so we generated Trim7 sufficient and deficient animals
169 both in the absence of STING. We orally inoculated STING^{Gt/Gt} Trim7^{+1/+1} or littermate
170 STING^{Gt/Gt} Trim7^{WT/+1} controls with MNV^{CW3} and assessed replication in the MLN, spleen,
171 liver, colon, or ileum via qPCR 7 days after infection. In each tissue, MNV genomes were
172 robustly detected but there were no significant differences between Trim7 sufficient and
173 deficient animals (**Figure 5A-5E**). These data demonstrate that removal of the STING
174 pathway in mice does not reveal a role for Trim7 in mediating MNV infection in vivo.

175

176 Trim7 has also been reported to target MAVS, an RNA sensing pathway that is also
177 responsible for regulating an innate immune response to MNV in vivo^{20,41,45}. Both MAVS
178 and STING converge upon type I and type III interferon (IFN) production which is a potent
179 inhibitor of MNV replication both in vitro and in vivo³¹. Therefore, to eliminate the potential
180 role of Trim7 regulating IFN induction, we crossed the Trim7^{+1/+1} mice onto a STAT1^{-/-}
181 background which eliminates all IFN signaling. STAT1 deficient mice are highly sensitive
182 to MNV and succumb to infection unlike immunocompetent animals^{12,28}. Trim7 sufficient
183 and deficient animals lacking STAT1 were orally inoculated with a 1000 PFU of MNV^{CW3}
184 and monitored for survival for 21 days. Deficiency of Trim7 did not affect the lethality
185 caused by MNV^{CW3} in these mice (**Figure 5F**). Taken together our data finds a lack of a
186 physiological role of Trim7 even in the absence of STING or STAT1.

187 **Discussion**

188 Trim7 has emerged as a core component of host-virus interactions with both pro-viral and
189 anti-viral activity based largely on compelling in vitro data. Due to the strong antiviral
190 action of Trim7 overexpression in vitro, we hypothesized that Trim7 might have an
191 important role in the clearance of MNV infection in vivo. However, our extensive studies
192 found no significant role for Trim7 in MNV restriction using Trim7 deficient mice and
193 different strains of MNV with distinct cellular and tissue tropisms. Trim7 deficiency did not
194 have any effect on acute infection with MNV^{CW3} in systemic tissues, nor did it have any
195 effect on persistent infection with MNV^{CR6} which primarily infects intestinal tuft cells.

196

197 MNV is efficiently controlled by the immune system and causes no symptomatic disease
198 in immunocompetent adult mice. Both the innate and adaptive immune systems are
199 necessary to clear infections¹². Trim7 has been reported to influence host innate immune
200 defenses due to its role in the degradation of STING and MAVS, leading to decreased
201 inflammatory response to infection^{20,21}. Thus, we tested the possibility that the
202 physiological function of Trim7 is primarily focused on cytokine and innate immune
203 responses rather than direct antiviral activity. In the context of acute MNV infection we did
204 not observe any changes in the induction of pro-inflammatory cytokines, which contrasts
205 with what others have reported for both DNA and RNA viruses^{20,21}. However, neither
206 STING nor MAVS have a C-terminal glutamine residue that has been structurally and
207 biochemically demonstrated by multiple groups to be the hallmark of a Trim7 substrate¹⁶⁻
208 ¹⁸. Thus it is possible that neither STING nor MAVS are direct targets of Trim7, but the
209 levels of these innate immune sensors are regulated indirectly by Trim7 in a context

210 dependent manner. In addition to the lack of change in cytokine responses in infected
211 mice lacking Trim7, we observe no impact of Trim7 on MNV infection patterns when
212 STING or STAT1 are removed.

213

214 While this current study utilized multiple orthogonal approaches to probe for a
215 physiological role for Trim7 in MNV infection, it does have several limitations. First, our
216 data does not exclude the possibility that Trim7 may have a role in regulating MNV
217 infections under very specific conditions that we did not test. Second, our data does not
218 speak to whether other viruses whose protein products contain C-terminal glutamines are
219 restricted by Trim7 in vivo. Lastly, our findings that the cytokine response to MNV
220 infections is unaffected by Trim7, which is contrary to the models in the literature, may be
221 a result of the specific virus we used or differences in the baseline physiology of our
222 animals due to unidentified differences in animal facilities. Nevertheless, despite
223 compelling evidence of the role of Trim7 in host defense in vitro, we see no physiological
224 evidence for its activity in MNV clearance. Thus, caution should be exerted when
225 classifying Trim7 as a broad acting antiviral recognizing the products of 3C-like protease
226 cleavage events.

227 **Materials and Methods**

228 **Mouse strains**

229 All mouse experiments were conducted at University of Texas Southwestern Medical
230 Center and approved by the University of Texas Southwestern Medical Center's
231 Institutional Animal Care and Use committees. C57BL/6J wild-type, C57BL/6J-Sting1gt/J
232 and Stat1^{-/-} [B6.129S(Cg)-Stat1tm1Div/J]³⁸ mice were originally purchased from Jackson
233 Laboratories and bred in-housed under specific pathogen-free conditions, including
234 devoid of murine norovirus. Two CRISPR KO lines for Trim7 deletion (BL6/Trim7^{+1/+1} and
235 BL6ΔTrim) were used for our experiments. Trim7^{+1/+1} line was previously described¹⁹, and
236 BL6ΔTrim7 line was made using the same strategy to create a larger deletion. Briefly, two
237 sgRNAs targeting exon 1 (AGGACACGGATGGCGACTGT) and exon 7
238 (AGTTGACGCGGAAGGTGTAG) of the mouse Trim7 were generated, and co-
239 microinjected with Cas9 mRNA into fertilized eggs of C57BL/6N mice¹⁹ (Figure 1A and
240 1B). Embryos were cultured overnight in M16 medium and were implanted into
241 pseudopregnant foster mothers after reaching the 2-cell stage of development. Offspring
242 were genotyped by PCR and sanger sequencing. Founder mice were bred with C57BL/6J
243 mice to establish respective lines. All experiments were performed with gender-balanced
244 littermate controls and independently replicated at least three times. Mice were used for
245 infections between 6–10 weeks of age. Genotyping of the mice was done by real time
246 PCR as described previously¹⁹.

247

248

249 **Western Blot**

250 Indicated tissues from uninfected mice (Trim7^{+1/+1} and Trim7^{Δ/Δ}) were collected, washed
251 in ice-cold phosphate-buffered saline (PBS) and homogenized in RIPA lysis buffer (25mM
252 Tris, 150mM NaCl, 1% IGEPAL, 0.5% sodium deoxycholate, 0.1% SDS) supplemented
253 with Halt™ protease inhibitor cocktail (Thermo Fisher Scientific) using a bead beater at
254 6800rpm for 1min. Homogenized samples were centrifuged at 13,000rpm for 20min at
255 4°C to remove cell debris. Protein concentrations of the supernatants were quantified
256 using Coomassie Plus (Bradford) Assay Reagent (Thermo Fisher Scientific) normalized
257 to a BSA standard curve on a BioTek Synergy LX Multimode Reader. Samples were then
258 diluted and boiled with 2x Laemmli Sample Buffer (BioRad). For a positive control we
259 used cell lysates overexpressing Trim7 isoforms. Lysates were resolved on SDS-PAGE
260 gels and transferred to PVDF membranes.

261 Western blot was performed using the following antibodies: anti-Trim7 antibody produced
262 in rabbit (Sigma SAB2106626; shown in **Figure 1B**), Trim7-antibody N-term (Abcepta
263 AP11979a-ev), Trim7 polyclonal antibody (Bioss BS-9164R), Trim7 antibody C-term
264 (GeneTex GTX24541), Anti-TRIM7 antibody produced in rabbit (Sigma HPA039213),
265 Monoclonal Anti-GAPDH-Peroxidase antibody produced in mouse (Sigma G9295) and
266 Anti-Mouse IgG (H+L), F(ab')₂ fragment peroxidase antibody in goat (Sigma
267 SAB3701122).

268

269 **MNV infections in mice**

270 MNV stocks were generated from plasmids encoding parental MNV^{CW3} (GenBank ID
271 EF014462.1) or parental MNV^{CR6} (GenBank ID JQ237823) as described previously³⁹.
272 Viral stocks were obtained from plasmids expressing the complete genome of the viruses
273 and purified and titered as previously described⁴⁰. Genetic identity of viral stocks was
274 confirmed by targeted sequencing.

275 Stocks of MNV^{CW3} P1 was diluted to 5×10^6 PFU per 25uL of DMEM (with 5% fetal bovine
276 serum) and inoculated per-orally in BL6/Trim7^{+1/+1}, BL6/Trim7^{Δ/Δ}, and BL6/Sting^{Gt/Gt}
277 Trim7^{+1/+1} mice that were littermate-matched. Mice were euthanized at 7 days post-
278 infection and mesenteric lymph nodes (MLN), spleen, liver, colon and ileum were
279 harvested for RNA isolation. BL6/Stat1^{-/-}Trim7^{+1/+1} mice and littermates were infected with
280 MNV^{CW3} at 1000 PFU per animal, singly housed and monitored daily for survival for 21
281 days. MNV^{CR6} was inoculated in BL6/Trim7^{+1/+1} and littermate controls at 1×10^6 PFU per
282 animal. Mice were singly housed immediately after infection. Fecal samples were
283 collected at days 3, 7, 14 and 21 post-infection. Mice were euthanized at 21 days post-
284 infection and indicated tissues were harvested for RNA isolation.

285

286 **RNA extraction and qPCR assays**

287 Quantification of MNV genomes from infected tissues was performed as previously
288 described⁴⁰. RNA was isolated from infected tissues using TRI Reagent (Sigma- Aldrich)
289 with a Direct-zol kit (Zymo Research) following the manufacturers' protocols. One μg of
290 RNA was used for cDNA synthesis using a High-Capacity cDNA Reverse Transcription
291 kit, following the manufacturer's protocols (Thermo Fisher Scientific). TaqMan quantitative

292 PCR (qPCR) for MNV was performed in triplicate on each sample and standard with
293 forward primer 5'-GTGCGCAACACAGAGAAACG-3', reverse primer 5'-
294 CGGGCTGAGCTTCCTGC-3', and probe 5'-6FAM-
295 CTAGTGTCTCCTTTGGAGCACCTA-BHQ1-3'. TaqMan qPCR for Actin was performed
296 in triplicate on each sample and standard with forward primer 5'-
297 GATTACTGCTCTGGCTCCTAG-3', reverse primer 5'-GACTCATCGTACTCCTGCTTG-
298 3', and probe 5'-6FAM-CTGGCCTCACTGTCCACCTTCC-6TAMSp-3'.

299 RNA from infected fecal pellets was isolated using RNeasy Mini QIAcube Kit (Qiagen)
300 and cDNA synthesis was performed using M-MLV Reverse Transcriptase kit (Invitrogen)
301 using manufacturers' protocols.

302 qPCR assays for cytokines and chemokines, and Trim7 were designed from IDT and the
303 assay was performed in triplicate on each sample and standards with forward primer,
304 reverse primer and probes as listed below:

305 Ifnb1: Probe: 5'-6-FAM/ ATCTCTGCTCGGACCACCATCC-6-TAMSp-3'

306 Primer 1: 5'- ACTCATGAAGTACAACAGCTACG -3'

307 Primer 2: 5'- GGCATCAACTGACAGGTCTT -3'

308 IL6: Probe: 5'-6-FAM/ CCTACCCCAATTTCCAATGCTCTCCT-6-TAMSp-3'

309 Primer 1: 5'- AGCCAGAGTCCTTCAGAGA -3'

310 Primer 2: 5'- TCCTTAGCCACTCCTTCTGT -3'

311 Ifit1: Probe: 5'-6-FAM/ ACAGCTACCACCTTTACAGCAACCAT-6-TAMSp-3'

312 Primer 1: 5'- GCAAGAGAGCAGAGAGTCAAG -3'

313 Primer 2: 5'- TGAAGCAGATTCTCCATGACC -3'

314 Cxcl10: Probe: 5'-6-FAM/ATCCCTCTCGCAAGGACGGTC-6-TAMSp-3'

315 Primer 1: 5'- ATTTTCTGCCTCATCCTGCT -3'

316 Primer 2: 5'- TGATTTCAAGCTTCCCTATGGC -3'

317 Trim7: Probe: 5'-6-FAM/ CCTCTGTTGACCGGAACGCTTCAT-6-TAMSp-3'

318 Primer 1: 5'- GTAGAGGGAGTTGCTGGATTC -3'

319 Primer 2: 5'- GCTGCCATCTGCTTCTGT -3'

320 These transcript levels were normalized to actin and indicated as fold change relative to
321 infected BL6/WT tissues.

322

323 **Acknowledgements**

324 We would like to thank John Schoggins and all members of the Orchard Lab for helpful
325 discussions. This work was supported by NIH grant 5R01DK133231 (R.C.O.). The work
326 was supported in part by the Division of Intramural Research, National Institutes of Health,
327 National Institute of Allergy and Infectious Diseases.

328

329 **Author Contributions**

330 M.A.S. designed the project, performed experiments and helped draft the paper. L.R.P.,
331 M.C.O. S.J.R., G.L.S. and S.M.B helped perform experiments and provided critical

332 reagents. R.C.O. conceptualized the project, provided supervision, and helped write the
333 paper. All authors read and edited the manuscript.

334 **Disclosures**

335 The authors have no financial disclosures.

336 References

337

- 338 1. Karst SM, Wobus CE, Goodfellow IG, et al. Advances in norovirus biology. *Cell*
339 *Host Microbe* 2014;15(6):668-80, doi:10.1016/j.chom.2014.05.015
- 340 2. Bartsch SM, O'Shea KJ, Wedlock PT, et al. Potential Clinical and Economic
341 Value of Norovirus Vaccination in the Community Setting. *Am J Prev Med*
342 2021;60(3):360-368, doi:10.1016/j.amepre.2020.10.022
- 343 3. Bartsch SM, O'Shea KJ, Lee BY. The Clinical and Economic Burden of Norovirus
344 Gastroenteritis in the United States. *J Infect Dis* 2020;222(11):1910-1919,
345 doi:10.1093/infdis/jiaa292
- 346 4. Schwartz S, Vergoulidou M, Schreier E, et al. Norovirus gastroenteritis causes
347 severe and lethal complications after chemotherapy and hematopoietic stem cell
348 transplantation. *Blood* 2011;117(22):5850-6, doi:10.1182/blood-2010-12-325886
- 349 5. Siebenga JJ, Beersma MF, Vennema H, et al. High prevalence of prolonged
350 norovirus shedding and illness among hospitalized patients: a model for in vivo
351 molecular evolution. *J Infect Dis* 2008;198(7):994-1001, doi:10.1086/591627
- 352 6. Ettayebi K, Crawford SE, Murakami K, et al. Replication of human noroviruses in
353 stem cell-derived human enteroids. *Science* 2016;353(6306):1387-1393,
354 doi:10.1126/science.aaf5211
- 355 7. Jones MK, Watanabe M, Zhu S, et al. Enteric bacteria promote human and
356 mouse norovirus infection of B cells. *Science* 2014;346(6210):755-9,
357 doi:10.1126/science.1257147
- 358 8. Estes MK, Ettayebi K, Tenge VR, et al. Human Norovirus Cultivation in
359 Nontransformed Stem Cell-Derived Human Intestinal Enteroid Cultures: Success and
360 Challenges. *Viruses* 2019;11(7), doi:10.3390/v11070638
- 361 9. Jones MK, Grau KR, Costantini V, et al. Human norovirus culture in B cells. *Nat*
362 *Protoc* 2015;10(12):1939-47, doi:10.1038/nprot.2015.121
- 363 10. Rimkute I, Chaimongkol N, Woods KD, et al. A non-human primate model for
364 human norovirus infection. *Nat Microbiol* 2024;9(3):776-786, doi:10.1038/s41564-023-
365 01585-7
- 366 11. Wobus CE, Karst SM, Thackray LB, et al. Replication of Norovirus in cell culture
367 reveals a tropism for dendritic cells and macrophages. *PLoS Biol* 2004;2(12):e432,
368 doi:10.1371/journal.pbio.0020432
- 369 12. Karst SM, Wobus CE, Lay M, et al. STAT1-dependent innate immunity to a
370 Norwalk-like virus. *Science* 2003;299(5612):1575-8, doi:10.1126/science.1077905
- 371 13. Baldrige MT, Turula H, Wobus CE. Norovirus Regulation by Host and Microbe.
372 *Trends Mol Med* 2016;22(12):1047-1059, doi:10.1016/j.molmed.2016.10.003
- 373 14. Orchard RC, Sullender ME, Dunlap BF, et al. Identification of Antinorovirus
374 Genes in Human Cells Using Genome-Wide CRISPR Activation Screening. *J Virol*
375 2019;93(1), doi:10.1128/JVI.01324-18
- 376 15. Skurat AV, Dietrich AD, Zhai L, et al. GNIP, a novel protein that binds and
377 activates glycogenin, the self-glucosylating initiator of glycogen biosynthesis. *J Biol*
378 *Chem* 2002;277(22):19331-8, doi:10.1074/jbc.M201190200
- 379 16. Ru Y, Yan X, Zhang B, et al. C-terminal glutamine acts as a C-degron targeted by
380 E3 ubiquitin ligase TRIM7. *Proc Natl Acad Sci U S A* 2022;119(30):e2203218119,
381 doi:10.1073/pnas.2203218119

- 382 17. Luptak J, Mallery DL, Jahun AS, et al. TRIM7 Restricts Coxsackievirus and
383 Norovirus Infection by Detecting the C-Terminal Glutamine Generated by 3C Protease
384 Processing. *Viruses* 2022;14(8), doi:10.3390/v14081610
- 385 18. Liang X, Xiao J, Li X, et al. A C-terminal glutamine recognition mechanism
386 revealed by E3 ligase TRIM7 structures. *Nat Chem Biol* 2022;18(11):1214-1223,
387 doi:10.1038/s41589-022-01128-x
- 388 19. Giraldo MI, Xia H, Aguilera-Aguirre L, et al. Envelope protein ubiquitination drives
389 entry and pathogenesis of Zika virus. *Nature* 2020;585(7825):414-419,
390 doi:10.1038/s41586-020-2457-8
- 391 20. Yang B, Zhang G, Qin X, et al. Negative Regulation of RNF90 on RNA Virus-
392 Triggered Antiviral Immune Responses Targeting MAVS. *Front Immunol*
393 2021;12(730483, doi:10.3389/fimmu.2021.730483
- 394 21. Yang B, Liu Y, Cui Y, et al. RNF90 negatively regulates cellular antiviral
395 responses by targeting MITA for degradation. *PLoS Pathog* 2020;16(3):e1008387,
396 doi:10.1371/journal.ppat.1008387
- 397 22. Fan W, Mar KB, Sari L, et al. TRIM7 inhibits enterovirus replication and promotes
398 emergence of a viral variant with increased pathogenicity. *Cell* 2021;184(13):3410-3425
399 e17, doi:10.1016/j.cell.2021.04.047
- 400 23. Fan W, McDougal MB, Schoggins JW. Enterovirus 3C Protease Cleaves TRIM7
401 To Dampen Its Antiviral Activity. *J Virol* 2022;96(19):e0133222, doi:10.1128/jvi.01332-22
- 402 24. Sullender ME, Pierce LR, Annaswamy Srinivas M, et al. Selective Polyprotein
403 Processing Determines Norovirus Sensitivity to Trim7. *J Virol* 2022;96(17):e0070722,
404 doi:10.1128/jvi.00707-22
- 405 25. Tsu BV, Beierschmitt C, Ryan AP, et al. Diverse viral proteases activate the
406 NLRP1 inflammasome. *Elife* 2021;10(doi:10.7554/eLife.60609
- 407 26. Grau KR, Zhu S, Peterson ST, et al. The intestinal regionalization of acute
408 norovirus infection is regulated by the microbiota via bile acid-mediated priming of type
409 III interferon. *Nat Microbiol* 2020;5(1):84-92, doi:10.1038/s41564-019-0602-7
- 410 27. Grau KR, Roth AN, Zhu S, et al. The major targets of acute norovirus infection
411 are immune cells in the gut-associated lymphoid tissue. *Nat Microbiol* 2017;2(12):1586-
412 1591, doi:10.1038/s41564-017-0057-7
- 413 28. Mumphy SM, Changotra H, Moore TN, et al. Murine norovirus 1 infection is
414 associated with histopathological changes in immunocompetent hosts, but clinical
415 disease is prevented by STAT1-dependent interferon responses. *J Virol*
416 2007;81(7):3251-63, doi:10.1128/JVI.02096-06
- 417 29. Nice TJ, Strong DW, McCune BT, et al. A single-amino-acid change in murine
418 norovirus NS1/2 is sufficient for colonic tropism and persistence. *J Virol* 2013;87(1):327-
419 34, doi:10.1128/JVI.01864-12
- 420 30. Nice TJ, Baldridge MT, McCune BT, et al. Interferon-lambda cures persistent
421 murine norovirus infection in the absence of adaptive immunity. *Science*
422 2015;347(6219):269-73, doi:10.1126/science.1258100
- 423 31. Ingle H, Makimaa H, Aggarwal S, et al. IFN-lambda derived from nonsusceptible
424 enterocytes acts on tuft cells to limit persistent norovirus. *Sci Adv* 2023;9(37):eadi2562,
425 doi:10.1126/sciadv.adi2562
- 426 32. Nice TJ, Osborne LC, Tomov VT, et al. Type I Interferon Receptor Deficiency in
427 Dendritic Cells Facilitates Systemic Murine Norovirus Persistence Despite Enhanced

- 428 Adaptive Immunity. *PLoS Pathog* 2016;12(6):e1005684,
429 doi:10.1371/journal.ppat.1005684
- 430 33. Lee S, Liu H, Wilen CB, et al. A Secreted Viral Nonstructural Protein Determines
431 Intestinal Norovirus Pathogenesis. *Cell Host Microbe* 2019;25(6):845-857 e5,
432 doi:10.1016/j.chom.2019.04.005
- 433 34. Strine MS, Fagerberg E, Darcy PW, et al. Intestinal tuft cell immune privilege
434 enables norovirus persistence. *Sci Immunol* 2024;9(93):eadi7038,
435 doi:10.1126/sciimmunol.adi7038
- 436 35. Van Winkle JA, Robinson BA, Peters AM, et al. Persistence of Systemic Murine
437 Norovirus Is Maintained by Inflammatory Recruitment of Susceptible Myeloid Cells. *Cell*
438 *Host Microbe* 2018;24(5):665-676 e4, doi:10.1016/j.chom.2018.10.003
- 439 36. Wilen CB, Lee S, Hsieh LL, et al. Tropism for tuft cells determines immune
440 promotion of norovirus pathogenesis. *Science* 2018;360(6385):204-208,
441 doi:10.1126/science.aar3799
- 442 37. Saito M, Goel-Apaza S, Espetia S, et al. Multiple norovirus infections in a birth
443 cohort in a Peruvian Periurban community. *Clin Infect Dis* 2014;58(4):483-91,
444 doi:10.1093/cid/cit763
- 445 38. Durbin JE, Hackenmiller R, Simon MC, et al. Targeted disruption of the mouse
446 *Stat1* gene results in compromised innate immunity to viral disease. *Cell*
447 1996;84(3):443-50, doi:10.1016/s0092-8674(00)81289-1
- 448 39. Strong DW, Thackray LB, Smith TJ, et al. Protruding domain of capsid protein is
449 necessary and sufficient to determine murine norovirus replication and pathogenesis in
450 vivo. *J Virol* 2012;86(6):2950-8, doi:10.1128/JVI.07038-11
- 451 40. Orchard RC, Wilen CB, Doench JG, et al. Discovery of a proteinaceous cellular
452 receptor for a norovirus. *Science* 2016;353(6302):933-6, doi:10.1126/science.aaf1220
- 453 41. McCartney SA, Thackray LB, Gitlin L, et al. MDA-5 recognition of a murine
454 norovirus. *PLoS Pathog* 2008;4(7):e1000108, doi:10.1371/journal.ppat.1000108
- 455 42. Brocard M, Lu J, Hall B, et al. Murine Norovirus Infection Results in Anti-
456 inflammatory Response Downstream of Amino Acid Depletion in Macrophages. *J Virol*
457 2021;95(20):e0113421, doi:10.1128/JVI.01134-21
- 458 43. Jahun AS, Sorgeloos F, Chaudhry Y, et al. Leaked genomic and mitochondrial
459 DNA contribute to the host response to noroviruses in a STING-dependent manner. *Cell*
460 *Rep* 2023;42(3):112179, doi:10.1016/j.celrep.2023.112179
- 461 44. Yu P, Miao Z, Li Y, et al. cGAS-STING effectively restricts murine norovirus
462 infection but antagonizes the antiviral action of N-terminus of RIG-I in mouse
463 macrophages. *Gut Microbes* 2021;13(1):1959839,
464 doi:10.1080/19490976.2021.1959839
- 465 45. Lazear HM, Lancaster A, Wilkins C, et al. IRF-3, IRF-5, and IRF-7 coordinately
466 regulate the type I IFN response in myeloid dendritic cells downstream of MAVS
467 signaling. *PLoS Pathog* 2013;9(1):e1003118, doi:10.1371/journal.ppat.1003118

468 **Figure 1. Overview of Trim7 deficient lines used in this study**

469 **A)** Cartoon of the mouse Trim7 locus. sgRNAs 1 and 2 were used to generate two Trim7
470 deficient mouse lines. Trim7^{+1/+1} has a one nucleotide insertion in exon 1 and has been
471 previously reported¹⁹. Trim7 Δ/Δ has a 12,373 nucleotide deletion between exons 1 and
472 7. Also marked are the qPCR primers and probe used for validation. qPCR primer 1 spans
473 the exon 1/2 junction.

474 **B)** Representative western blot of Trim7 of heart tissue from the indicated mouse lines
475 demonstrating a lack of specific band at the predicted molecular weight of Trim7 isoforms.

476 **C)** Trim7 expression from indicated tissues from wild-type BL6 mice as measured by
477 qPCR and normalized by concurrent quantification of actin transcripts. Dotted line
478 represents the limit of detection and each dot represents an individual mouse.

479 **D)** Trim7 expression in leg muscle relative to wild-type mice after normalization of actin
480 values. Each dot represents an individual mouse.

481

482 **Figure 2. Trim7 does not impact the replication or spread of acute murine norovirus**
483 **infection *in vivo*.**

484 C57BL/6-Trim7^{+1/+1} mice **(A)** or C57BL/6-Trim7^{Δ/Δ} mice **(B)** and respective littermate
485 controls were inoculated with 5×10^6 PFU of MNV^{CW3} and euthanized 7 days post-
486 infection. Tissue titers for mesenteric lymph nodes (MLN), spleen, liver, colon, and ileum
487 were analyzed via qPCR for MNV genome copies and normalized to actin.

488 **Figure 3. Trim7 does not impact the replication or spread of persistent enteric MNV**

489 C57BL/6-Trim7^{+1/+1} mice and littermate controls were inoculated with 1×10^6 PFU of
490 MNV^{CR6} and MNV genome copies were enumerated from fecal samples 3, 7, 14, or 21
491 days-post infection via qPCR **(A)**. 21 days post-infection, animals were sacrificed and
492 MNV burden assed by measuring the genome copies in the MLN **(B)**, colon **(C)**, ileum
493 **(D)**, spleen **(E)**, and liver **(F)** via qPCR. All samples were normalized relative to actin. Data
494 are shown as mean \pm S.D. from three independent experiments with 3-9 mice per group.
495 ns, ** $P < 0.01$, *** $P < 0.001$, **** $P < 0.0001$, Mann-Whitney's test.

496 **Figure 4. Trim7 does not affect innate immune response to MNV^{CW3} infection.**

497 C57BL/6-Trim7^{+1/+1} mice and littermate controls were inoculated with 5×10^6 PFU of
498 MNV^{CW3} and euthanized 7 days post-infection and indicated tissues were collected. **(A)**
499 Ifnb1, **(B)** IL6, **(C)** Ifit1 and **(D)** Cxcl10 transcript copies were determined via qPCR and
500 normalized to actin levels. The data are plotted relative to the average of the quantities in
501 WT mice post-MNV infection. Data are shown as mean \pm S.D. from three independent
502 experiments with 4-9 mice per group. ns, ** $P < 0.01$, *** $P < 0.001$, **** $P < 0.0001$, one-
503 way ANOVA with Tukey's multiple comparison test.

504 **Figure 5. STING and STAT1 dependent innate pathways do not mask the role of**
505 **Trim7 in restricting MNV^{CW3} infection.**

506 **A-E)** C57BL/6-Sting^{Gt/Gt} Trim7^{+1/+1} or littermate C57BL/6-Sting^{Gt/Gt} Trim7^{WT/+1} were
507 inoculated with 5×10^6 PFU of MNV^{CW3} and 7 days post-infection animals were sacrificed
508 and MNV burden assed by measuring the genome copies in the MLN (**A**), spleen (**B**),
509 liver (**C**), colon (**D**), and ileum (**E**) via qPCR. MNV genome levels were determined by
510 qPCR and normalized relative to actin transcripts. Data are shown as mean \pm S.D. from
511 three independent experiments with 11-12 mice per group. ns, ** $P < 0.01$, *** $P < 0.001$,
512 **** $P < 0.0001$, Mann-Whitney's test.

513 **F)** STAT1^{-/-} Trim7^{+1/+1} and littermate control mice were inoculated with 1×10^3 PFU of
514 MNV^{CW3} and monitored daily for survival for 21 days post-infection (12-13 mice per
515 group). Data from five independent experiments, analyzed using log-rank Mantel-Cox
516 test.

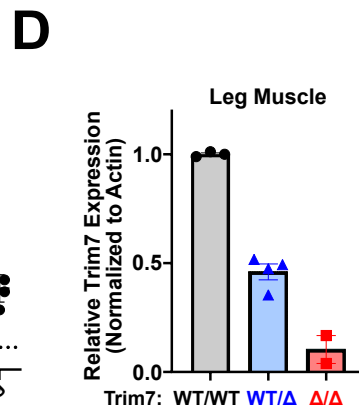
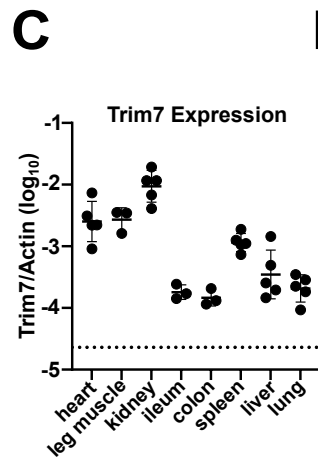
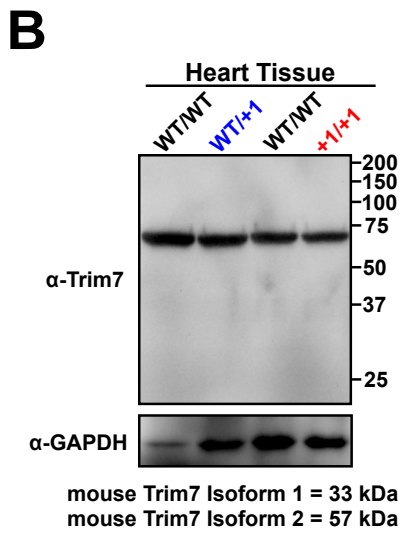
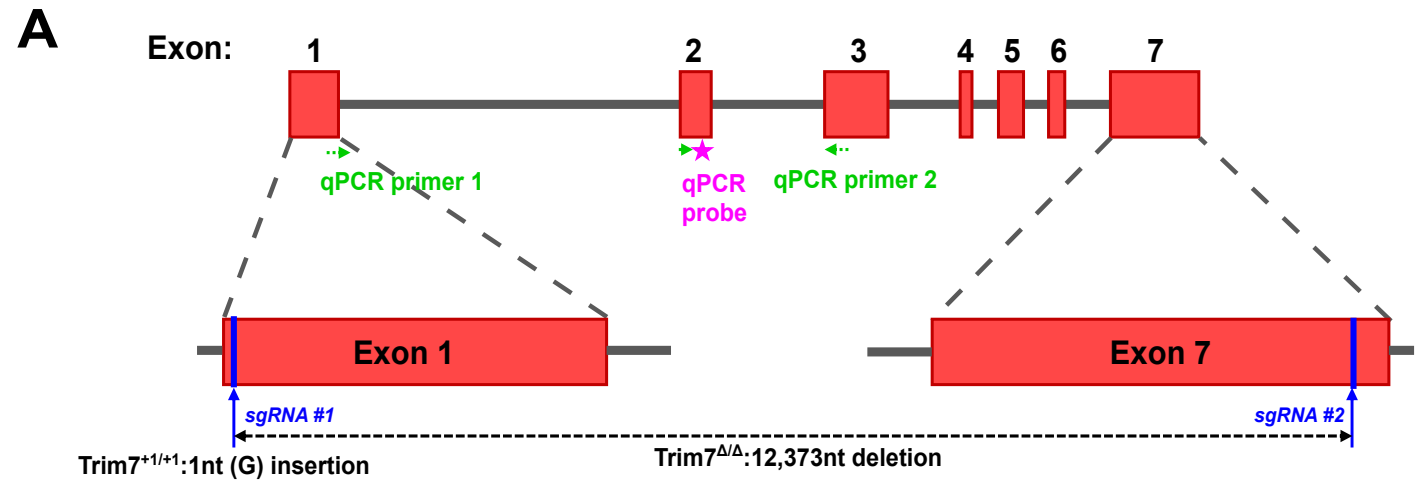
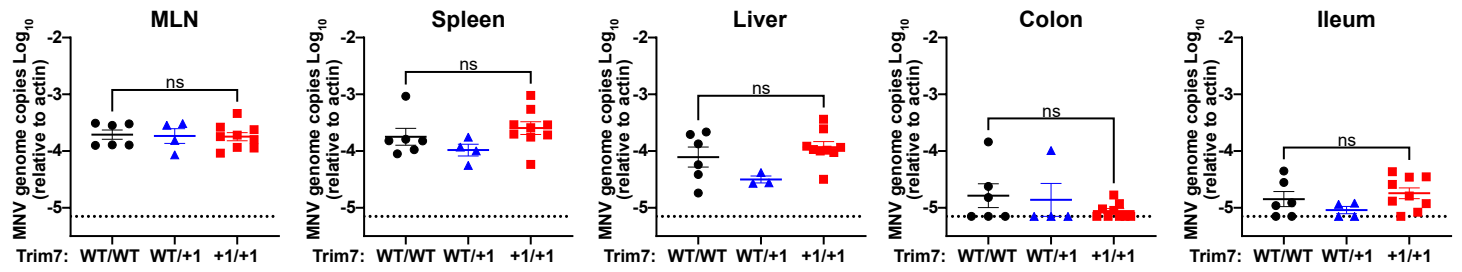


Figure 2

A



B

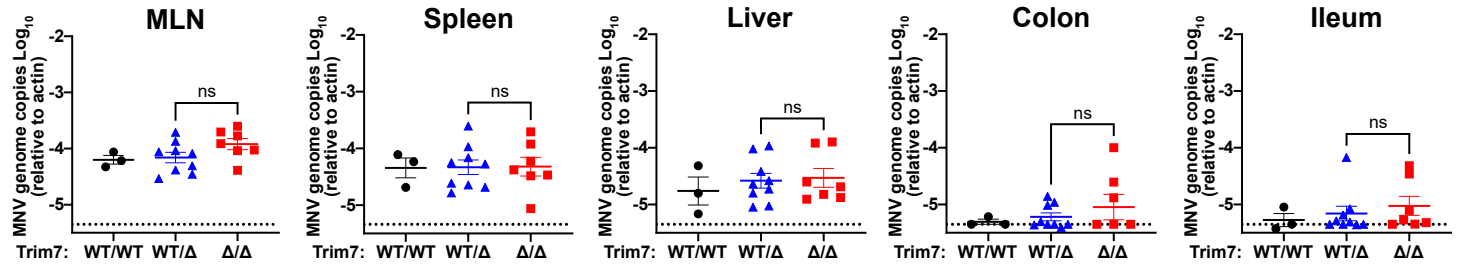
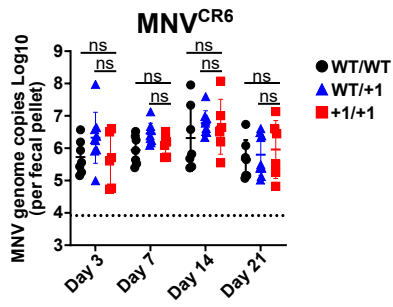


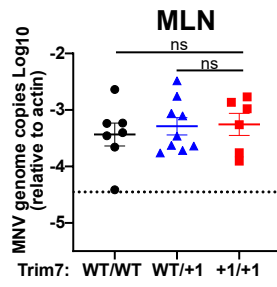
Figure 3

bioRxiv preprint doi: <https://doi.org/10.1101/2024.10.17.618898>; this version posted October 17, 2024. The copyright holder for this preprint (which was not certified by peer review) is the author/funder, who has granted bioRxiv a license to display the preprint in perpetuity. It is made available under aCC-BY-NC-ND 4.0 International license.

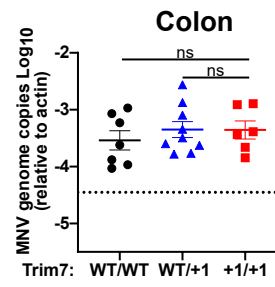
A



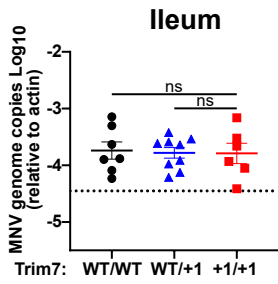
B



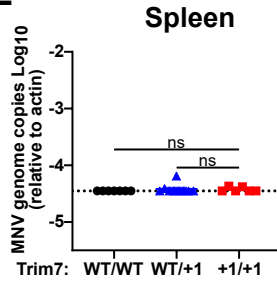
C



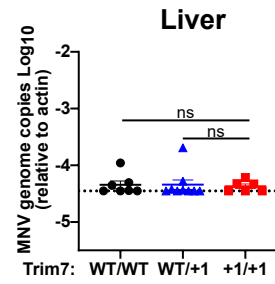
D



E



F



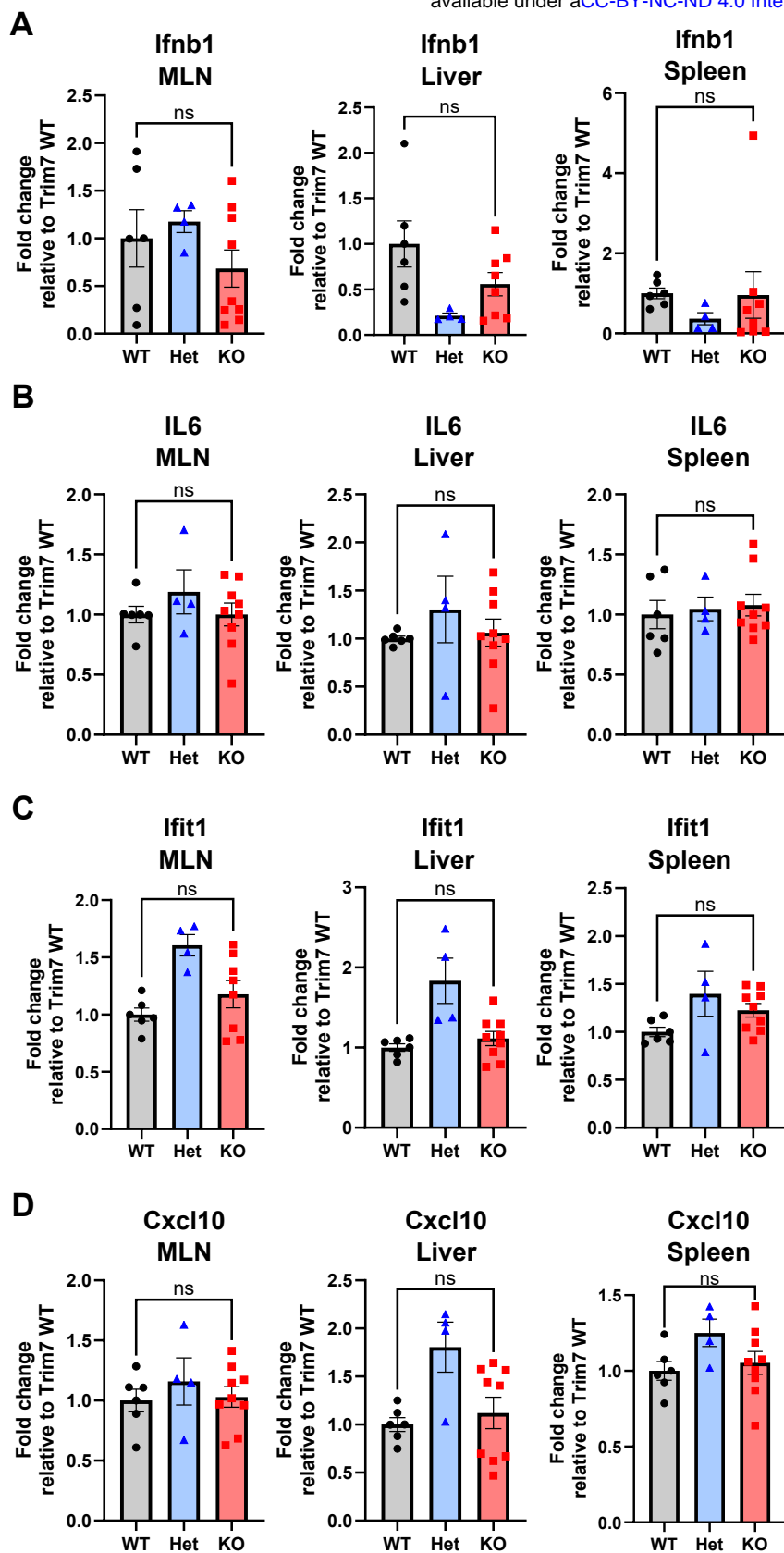


Figure 5

